

APPLICATION OF MATHEMATICAL MODELING AND PHYSICO-CHEMICAL ANALYSIS METHODS IN THE PREDICTION OF BIOLOGICAL ACTIVITY AND QUALITY CONTROL OF GOSSYPOL DERIVATIVES

ELENA V. USPENSKAYA* , POLYNA A. ZABORKINA , EVGENIYA A. RYNDINA , TATYANA V. PLETENEVA ,
MARIYA A. MOROZOVA , ILAHA V. KAZIMOVA , ANTON V. SYROESHKIN 

Department of Pharmaceutical and Toxicological Chemistry, Peoples Friendship University of Russia (RUDN University), 6 Miklukho-Maklaya St, Moscow, 117198, Russian Federation

*Email: uspenskaya75@mail.ru

Received: 02 Aug 2022, Revised and Accepted: 09 Sep 2022

ABSTRACT

Objective: The purpose of this work was to evaluate *in silico* biological activity profiles of real and virtual molecular structures of gossypol derivatives and to develop methods of Physico-chemical analysis to control their quality.

Methods: Substance of gossypol-acetic acid (GAA) and 14 virtual derivatives; PASS and ChemicDescript QSAR methods; low angle and dynamic laser light scattering (LALLS, DLS) methods; IR Spectroscopy–Cary 630 Fourier Transform IR Spectrometer, UV spectrometry–Cary-60 spectrophotometer, Optical microscopy (Altami BIO 2 microscope); *Spirotox* method for a sample's biological activity.

Results: A distance-based topological Balaban index (J) was successfully selected by ChemicDescript analysis; the P_a meaning by PASS Online program showed maximum (from 0.8 to 0.9) variations of antitumor and antiandrogenic and minimum of antiviral activities of GAA derivatives ($P_a < 0.5$) despite the existing literature data. Microscopy and DLS methods demonstrated the values of high powder dispersion $d = 0.8$ nm and weak stability of colloidal particles $\xi = -0.9$ mV. According to UV data $E_{1\text{cm}}^{1\%} = 42.4 \pm 0.8$ ($100 \text{ ml} \cdot \text{g}^{-1} \cdot \text{cm}^{-1}$) at $\lambda_{\text{max}} = 380$ nm. The LALLS method determined the GAA dissolution rate constant in ethanol: $k = 0.041 \pm 0.004 \text{ s}^{-1}$. The calculated activation energy values of cell biosensor death process in 1 mmol solution of GAA in *N,N*-DMF: ${}^{\circ}\text{bs}E_a = 174.36 \pm 0.45 \text{ kJ} \cdot \text{mol}^{-1}$ in comparison with the solvent medium: ${}^{\circ}\text{bs}E_a = 213 \pm 1.55 \text{ kJ} \cdot \text{mol}^{-1}$

Conclusion: The developed approach of chemometric, laser and biotesting methods can be used for the identification of biologically active properties, as well as for qualitative analysis within the development of the standard for the pharmaceutical substance of natural polyphenols.

Keywords: Gossypol-acetic acid, *In silico* methods, P_a/P_i ratios, Quality control, Analysis of physical and chemical properties

© 2022 The Authors. Published by Innovare Academic Sciences Pvt Ltd. This is an open access article under the CC BY license (<https://creativecommons.org/licenses/by/4.0/>)
DOI: <https://dx.doi.org/10.22159/ijap.2022v14i6.46052>. Journal homepage: <https://innovareacademics.in/journals/index.php/ijap>

INTRODUCTION

The natural polyphenol gossypol contained in cotton (genus *Gossypium*, family *Malvaceae*) is of great interest in pharmacy due to the high biological activity detected in this natural compound [1, 2]. Gossypol was discovered by Longmore and Marchlewski at the turn of the 19th and 20th centuries, having purified it by precipitation from an essential solution using acetic acid [3]. Adams *et al.* elucidated

and reported the gossypol-acetic acid structure as a 1',6',6',7,7' - hexahydroxy-3,3'-dimethyl-5,5'-disopropyl-(2,2'-binaphthalene)-8,8'-dicarboxaldehyde ($\text{C}_{32}\text{H}_{34}\text{O}_{10}$, $\text{Mr} = 578.6$). Gossypol, characterized by a rich yellow color due to a long conjugation chain, was positioned as an industrial dye; however, it demonstrated significant instability in the light. Later it was found that its instability is not due to molecular decomposition but to the existence of three tautomeric keto-enol forms in equilibrium (fig. 1).

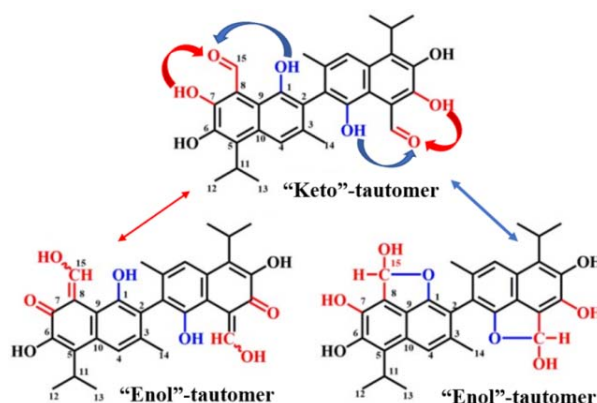


Fig. 1: The keto-enol tautomerization equilibrium of gossypol [4]

As can be seen in fig. 1 gossypol is an asymmetrical molecule and has restricted rotation around the binaphthyl bond. Therefore, enantiomers with different biological activity exist [5].

As a sesquiterpenoid and polyphenol, gossypol exhibits the properties of a polybasic-OH acid ($\text{pKa}_1 = 6.73$; $\text{pKa}_2 = 7.38$; $\text{pKa}_3 = 11.82$; $\text{pKa}_4 = 12.68$; $\text{pKa}_5 = 13.89$) and is capable of forming

azomethines (Schiff bases), oxidation, methylation products, etc. with different biological activity [6]. Numerous biological effects of gossypol on cell lines, animals and humans have been claimed: hypolipidemic, antibacterial, antiparasitic, antiviral, antitumor action [7-9]. The authors [10] characterize gossypol as a promising substance in the development of drugs for diseases such as resistant tumors, HIV, malaria, and psoriasis. However, its use in medicine is limited due to toxicity [11], insufficient accumulated data on the mechanisms of action, as well as the lack of existing techniques to assess authenticity, purity and content [12].

The present work is aimed on *in silico* methods application to predict the biological activity of gossypol derivatives and the development of Physico-chemical analysis techniques for gossypol-acetic acid (GAA) quality control.

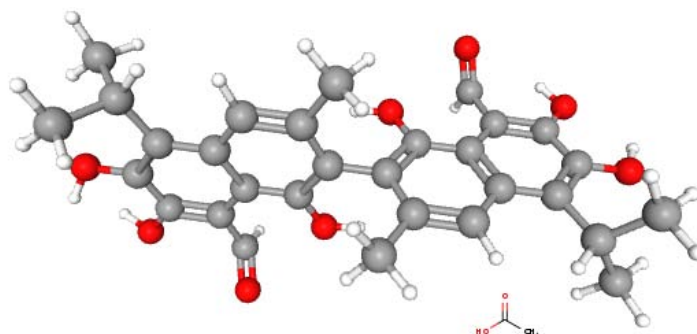


Fig. 2: Structure of gossypol-acetic acid (GAA) [14], real molecular structure of GAA: 7-(8-formyl-1,6,7-trihydroxy-3-methyl-5-propan-2-yl)naphthalen-2-yl)-2,3,8trihydroxy-6-methyl-4-propan-2-yl)naphthalene-1-carbaldehyde

Methods of research

To select "candidate substances", we used QSAR (Quantitative Structure-Activity Relationships) modeling-a procedure for constructing models of structures to predict their properties. We used ChemicPen software to construct and then save VMS in .chp and .mol formats and ChemDesc to work with Wiener, Rouvray, Balaban, bypass and electropathy topological indices [15-18].

In silico modelling: PASS (Prediction of Activity Spectra for Substances) Online [19], was used to predict the biological activity of loaded VMS using the criteria of P_a (probability to be active) and P_i (probability to be inactive) [16]. The ratio $P_a/P_i > 1$ was taken as the maximum value of activity; while the quantitative value of the property, close to zero ($P_a/P_i \rightarrow 0$), was considered as "not active".

The GAA analysis in the mid-infrared region was carried out using an Agilent Cary 630 FTIR spectrophotometer with a diamond ATR accessory (Agilent Technologies, USA). The spectral range is 4000–750 cm^{-1} . The resolution is less than 2 cm^{-1} , the correctness of the wave number is 0.05 cm^{-1} , the reproducibility of the wave number is 0.005 cm^{-1} . The thickness of the absorbing layer is 1.5 nm (the clamping device guarantees the setting of an optimal and reproducible pressure).

The optical density of GAA solutions in *N, N*-DMF in the UV region was measured on a Cary-60 spectrophotometer (Agilent Technologies, USA).

The GAA particles size and shape were determined by the optical microscopy method (microscope Altami BIO 2, Russia) with a 10-fold increase.

Kinetic dissolution of the GAA in ethanol was carried out by the method of low-angle laser light scattering (LALLS) [20] on Mastersizer 3600 optical set-up (Malvern Panalytical, United Kingdom) (fig. 3).

A 30-second background measurement was made prior to adding the examined disperse system to account for electrical background and scattering from the optics and 'clean' dispersant. The measurement of Laser Obscuration Time (LOT) was started while

MATERIALS AND METHODS

Powder substance

In this work, gossypol-acetic acid (GAA) produced by the Shemyakin and Ovchinnikov Institute of Bioorganic Chemistry (the content of API ≥ 97 , 5%) is presented in a real (fig. 2) and virtual molecular structures (RMS, VMS, respectively) of gossypol derivatives [13].

Sample preparation

The solvents—*N, N*-dimethylformamide anhydrous, 99.8% (DMF), ethanol 96% (Sigma-Aldrich, USA); deionized high resistance water (18.2 $\text{M}\Omega\cdot\text{cm}$ at 25 °C, Milli-Q system); chloroform (anhydrous, $\geq 99\%$), acetone (reagent, $\geq 99.5\%$)—were used to evaluate the solubility of GAA under equilibrium and kinetic conditions.

adding water to the cell and continued with 10 s intervals until complete dissolution of the sample with no more change of the examined parameter.

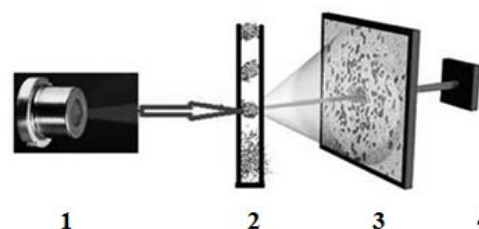


Fig. 3: Optical set-up of kinetic dissolution test. 1-He-Ne laser 632.8 nm; 2-capacity cell with examined disperse system; 3-diffraction pattern; 4-detector [21]

Spirotox method

Research of GAA biological activity was carried out with the use of test culture *Spirostomum ambiguum*, characterized by statistically reliable sensitivity to toxicants. The kinetic scheme of ligand-induced death of *S. ambiguum* is well described in [22]. The dependence of test culture lifetime ($t_{L,s}$) on temperature (T,K) was linearized in "Arrhenius coordinates" [23, 24]:

$$k = A \cdot e^{-E_a/RT}$$

Statistics

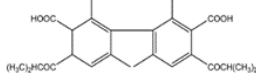
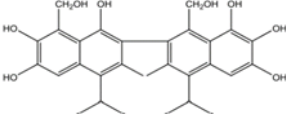
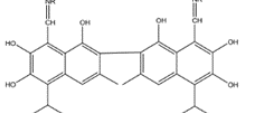
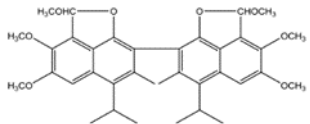
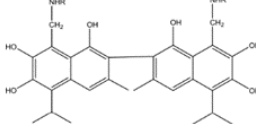
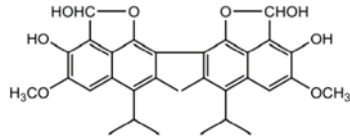
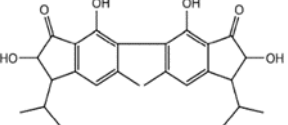
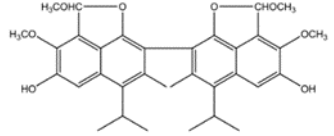
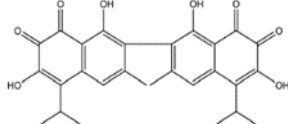
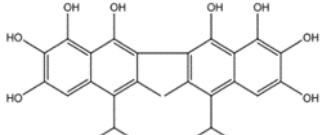
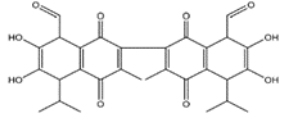
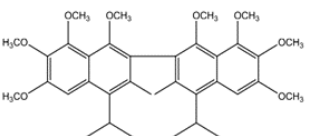
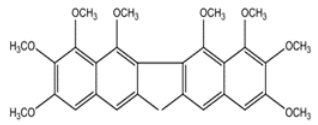
All obtained results were processed by statistical methods using software packages of OriginPro 2017. Each value in the fig. represents "mean \pm SD"; significant differences were considered when $p < 0.05$.

RESULTS AND DISCUSSION

In silico research

The fourteen structures of VMS of GAA constructed using ChemicDescript software are presented in table 1 [25].

Table 1: Gossypol derivatives-virtual related chemical structures

RMS of gossypol (fig. 2)		VMS of gossypol derivatives (by chemic descript)	
Nº	Molecular structures	Nº	Molecular structures
	Name Structure		Name Structure
1	Gihypolic acid 	8	Methanol derivative 
2	Imine-the Schiff base 	9	Hexamethyl ether 
3	Secondary amine 	10	Dimethyl ether 
4	Gossiden 	11	Tetramethyl ether 
5	Gossypol-o-binaftoketon 	12	Apogossypol 
6	Gossypolom 	13	Hexamethyl ether of apogossypol 
7	Methyl-derivative 	14	Hexamethyl ether of diisopropyl apogossypol 

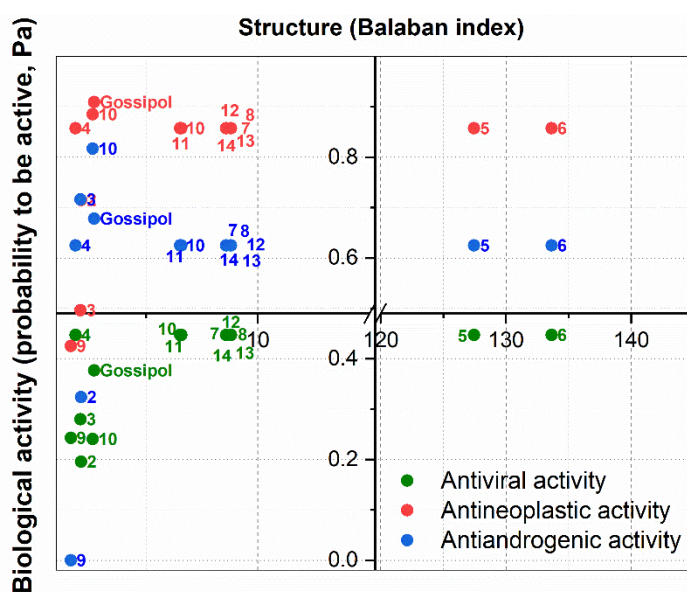


Fig. 4: The structure-activity ratio between balaban index and predicted properties of activity for gossypol derivatives, expressed in Pa: red-antitumor; blue-antiandrogenic; green-antiviral. The fig. in the diagram correspond to the GAA VMS from table 1

QSAR screening of VMS made it possible to choose one of five topological indices-distance-based Balaban index (J), reflecting the most significant differences for this type of compound with a certain activity, topology and geometry [26]. With the help of PASS Online product, we analyzed the quantitative values of the activity expressed in P_a probabilities. Fig. 4 shows a two-dimensional diagram of "structure-property" correlations for the most significantly manifested indicators of biological activity: antitumor (antagonism of the apoptosis regulator Bcl2), antiandrogenic (induction of azoospermia) and antiviral.

Analysis of the obtained diagrams showed that for most VMS, as well as for RMS of GAA, in fig. 4, the values of antitumor activity are as close as possible to "1" (P_a from 0.8 to 0.9), which may indicate a high probability of a positive effect when using GAA derivatives as part of antitumor agents [27]. A review of scientific publications and the results of experiments conducted in China [28] indicate the ability of drugs containing Gossypol to suppress spermatogenesis, causing azoospermia. Our QSAR study confirmed the literature data:

the probability to be active (P_a) for the majority (the exception are VMS 2 and 9) of gossypol derivatives was in the range from 0.6 to 0.8 (blue circles in see fig. 4). According to the analysis of the literature data [29], Gossypol has antiviral properties against HIV, influenza and other diseases. The results of our studies demonstrate the mutual correspondence of the Balaban index and the P_a indicator in fig. 4 with the absence of significant activity of this property in 15 representatives of VMS-values of $P_a \leq 0.5$.

Physico-chemical research

Description of GAA

The GAA substance solubility was evaluated in different solvents (table 2), which made it possible to determine the purity and consequently prognose the rate of release of the active pharmaceutical ingredient (API) from the finished dosage form, its absorption into the bloodstream and the achievement of a therapeutic effect [30].

Table 2: Solubility of GAA substance in various solvents

Solvent	Approximate volume of solvent in millilitres per gram of solute	Descriptive term
Acetone	from 1 to 10	Freely soluble
Chloroform	from 30 to 100	Sparingly soluble
Ethanol	from 100 to 1000	Slightly soluble
Water	more than 10 000	Slightly soluble

The observed differences in the solvent solubility indicate the high lipophilicity of GAA pharmaceutical substance (fig. 2).

The shape of substance particles plays a significant role for the proper quality of manufactured dosage forms, including such parameter as the release of API (fig. 5).

Microscopy results showed that GAA particles are irregularly shaped, with sharp corners and smooth surface, and mostly highly dispersed. The predominance of fine particles facilitates the release of API from the dosage form, and, taking into account the lipophilicity of gossypol $\log P=8.2$ also increases bioavailability [31].

The high dispersion of the GAA powder and the low colloidal stability were confirmed by the DLS method according to the parameters: size distribution, polydispersity index (PDI), average scattering light intensity (in kilo counts per second, kcps) and ζ -potential (table 3).



Fig. 5: Visualization of particles (size and shape) and granulometric composition (on the insert) of GAA by optical microscopy

Table 3: Characterization of nanoparticles in polyelectrolyte dispersions

Sample	C, g ml^{-1}	Size \pm SD, nm	PDI \pm SD	Count rate kcps,	$\bar{\xi} \pm$ SD, mV
Gossypol-acetic acid in ethanol	$3.0 \cdot 10^{-4}$	0.8 ± 0.2	0.36 ± 0.01	271	-0.9 ± 8

mean \pm SD, n=5, P=0.95

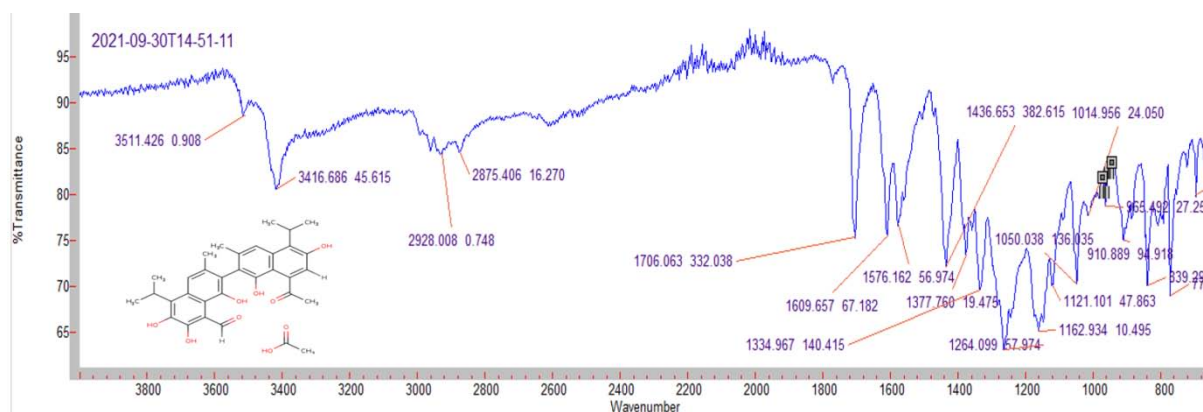


Fig. 6: IR spectra of GAA substance

Fourier transform infrared (FT-IR) spectroscopy

The vibrational-rotational spectrum of the GAA substance obtained by the ATR technique is shown in fig. 6.

The analysis of the IR spectrum showed the presence of characteristic light transmission bands corresponding to vibrations of bonds between atoms in the structural fragments of alcohol and phenolic hydroxyls, carbonyls, and numerous methylene groups (table 4).

Table 4: The main transmittance bands in the IR spectrum of GAA substance

Frequency range, cm^{-1}	Group	Compound class	Appearance/Comments
3550-3200	O-H stretching	alcohol	strong, broad/
3100-3000	C-H stretching	alkene	medium
1690-1640	C=O stretching	conjugated ketone	strong
1650-1566	C=C stretching	cyclic alkene	medium
1450	C-H bending	alkane	methyl group
1390-1310	O-H bending	phenol	medium
1085-1050	C-O stretching	primary alcohol	strong

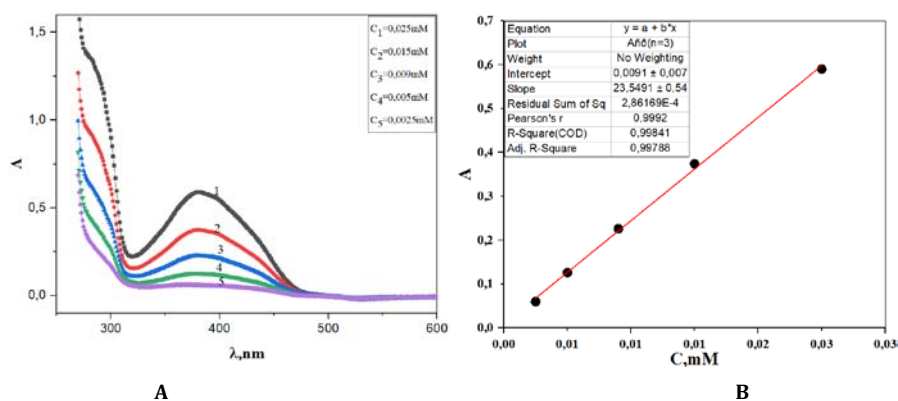
Thus, the results of FT-IR spectroscopy analysis allowed to propose this method as the first identification technique to characterize the investigated compound.

Ultraviolet-visible spectroscopy

Electronic spectra of GAA solutions in *N,N*-DMF exhibited characteristic absorption maximum at 380 nm, rising with concentration change from $2.5 \cdot 10^{-6}$ to $2.5 \cdot 10^{-5}$ $\text{mmol} \cdot \text{L}^{-1}$. This

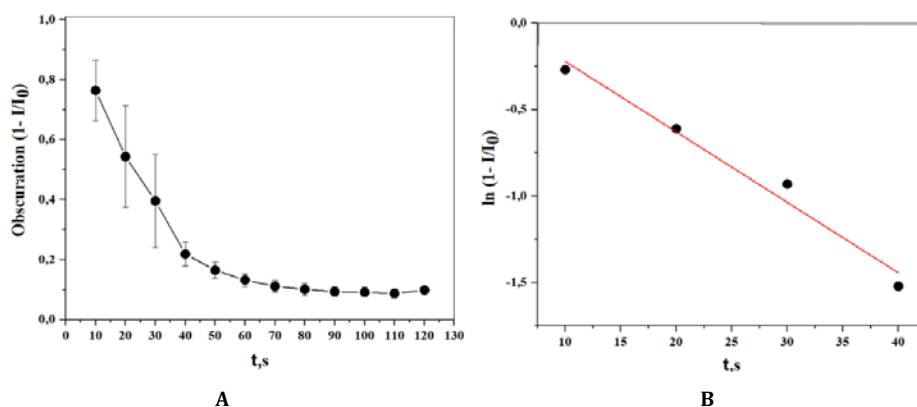
allowed not only identify the samples but also made the calibration curve for API assay using linear regression analysis (fig. 7).

The results of the UV method allowed us to calculate the specific absorption coefficient for a series of GAA solutions and use it to determine the identity of the GAA substance. The specific absorption coefficient $E_{1\text{cm}}^{1\%} = 42.4 \pm 0.8$ ($100 \text{ mg} \cdot \text{L}^{-1} \cdot \text{cm}^{-1}$) was also calculated at $\lambda_{\text{max}} = 380 \text{ nm}$, and mean error $\bar{\epsilon} = 0.02\%$ ($n=5, P=0.95$) (table 5).

**Fig. 7: UV spectra of GAA solutions in *N,N*-DMF in the concentration range from $2.5 \cdot 10^{-6}$ to $2.5 \cdot 10^{-5}$ $\text{mmol} \cdot \text{L}^{-1}$ (A); calibration line (B)****Table 5: The specific absorption coefficient of GAA in *N,N*-DMF**

$C \cdot 10^{-5}, \text{mol} \cdot \text{L}^{-1}$	\bar{A} (at $\lambda_{\text{max}} = 380 \text{ nm}$)	$E_{1\text{cm}}^{1\%}$ ($100 \text{ mg} \cdot \text{L}^{-1} \cdot \text{cm}^{-1}$)
2,5	0.060	41.4
5	0.126	43.5
9	0.226	43.3
15	0.374	43.0
25	0.590	40.7

$n=5, P=0.95$

**Fig. 8: Determination the dissolution rate of GAA: dependence of LO values on time in dispersed GAA ethanol solution depicted in linear (A) and semi-log coordinates (B), ($n=5; P=0.95$)**

Dissolution kinetics

The kinetic of GAA dissolution based on light scattering indicatrix registered in time was used to determine the Laser Obscuration (LO) values: $LO = 1 - I/I_0 \cdot 100\%$. Fig. 8 depicts the dependence of OL from the time during which GAA substance was dissolved in ethanol.

The kinetics of API's dissolution in ethanol turned out to be a two-step process: a sharp decrease in the recorded LO parameter from the onset of dissolution (first stage) was replaced by gradual decrease in the LO value until the plateau (second stage). We fixed it

as complete dissolution of the substance. The first stage was the speed-determining. We calculated the values of the constant dissolution rate for log-linearization as $k = -\text{tg}\alpha = 0,041 \text{ s}^{-1}$. The calculated dissolution rate constant can be used to characterize the identity of GAA in quality control and standardization process [32].

Spirotox

To estimate the biological activity of GAA substance, the temperature dependence of *S. ambiguus* death in the range of 295-303 K in increments of 2 K was analyzed (fig. 9).

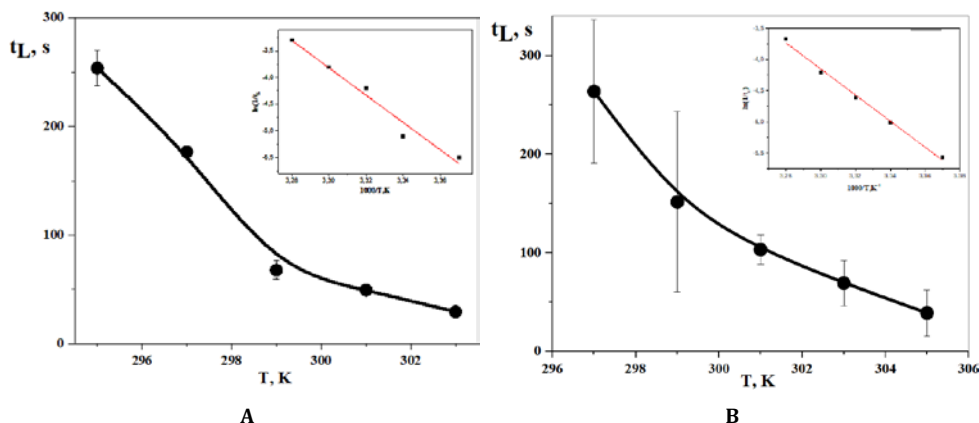


Fig. 9: Dependence of life span of *S. ambiguus* on temperature in the control *N,N*-DMF: water 1:30 solution (A) and in 1 mmol solution of GAA in *N,N*-DMF: water 1:30 (B) in linear and Arrhenius (on inserts) coordinates ($n=5$, $P=0.90$)

Table 6: The calculated ${}^{\text{obs}}E_a$ values of ligand-induced *S. ambiguus* death process in control *N,N*-DMF: water 1:30 solution and 1 mmol solution of GAA in *N,N*-DMF: water 1:30

Sample	${}^{\text{obs}}E_a \pm \text{SD}, \text{kJ} \cdot \text{mol}^{-1}$
<i>N,N</i> -DMF: water solution (1:30)–control solution	213.4 ± 1.5
1 mmol <i>N,N</i> -DMF: water solution (1:30)–test solution	174.2 ± 0.5

mean \pm SD, $n=5$, $P=0.90$

The observed activation energy (${}^{\text{obs}}E_a$) values for test and control solutions were found using Arrhenius coordinates (table 6).

The value of ${}^{\text{obs}}E_a$ reflects the ligand-receptor interaction accompanied by cell death. The lower activation energy, as well as the reduction of *S. ambiguus*'s lifetime by about 1.2 times at the same temperature for control *N,N*-DMF: water solution compared to 1 mmol GAA in *N,N*-DMF, indicates a higher biological activity/toxicity of the nature polyphenol compound [33].

CONCLUSION

An integrated approach to the study of the structure and properties of natural polyphenol originating from the cotton plant (*Gossypium*), based on an *in silico* approach and analytical techniques, allowed not only give the substance a complete characteristic for the purpose of standardization but also to predict its biological activity for the development of ready-made targeted drugs.

FUNDING

This paper has been supported by the RUDN University Strategic Academic Leadership Program.

AUTHORS CONTRIBUTIONS

All the authors have contributed equally

CONFLICT OF INTERESTS

The authors declare no other conflict of interest.

REFERENCES

1. Liu Y, Wang L, Zhao L, Zhang Y. Structure, properties of gossypol and its derivatives-from physiological activities to

- drug discovery and drug design. Nat Prod Rep. 2022;39(6):1282-304. doi: 10.1039/d1np00080b, PMID 35587693.
- Zhi-Ming D, Yang-Wu C, Yong-Sheng W, Muhammad JA, Sheng-Ji Y, Ze-Qun D. Gossypol exposure induces mitochondrial dysfunction and oxidative stress during mouse oocyte *in vitro* maturation. Chem Biol Interact. 2021;348(6):109-42.
 - He Z, Nam S, Zhang H, Olanya OM. Chemical composition and thermogravimetric behaviors of Glanded and glandless cottonseed kernels. Molecules. 2022;27(1):316-26. doi: 10.3390/molecules27010316, PMID 35011547.
 - Wang L, Liu Y, Zhang Y, Yasin A, Zhang L. Investigating stability and tautomerization of gossypol-A spectroscopy study. Molecules. 2019;24(7):1286-97. doi: 10.3390/molecules24071286, PMID 30987000.
 - Pardeshi M, Deshmukh A, Gajare K. Ruellia tuberosa linn. acts as an anti-fertility agent that reduces sperm count, motility and viability in male swiss albino mice (mus-musculus). Int J Curr Pharm Sci. 2016;9(8):105-9.
 - Gadella IC, Fonseca NB, Oloris SC, Melo MM, Soto-Blanco B. Gossypol toxicity from cottonseed products. Scientific World Journal. 2014;2014:231635. doi: 10.1155/2014/231635. PMID 24895646.
 - El-Lakkany NM, Elkattan HH, Elsisy AE. The ponatinib/gossypol novel combination provides enhanced anticancer activity against murine solid Ehrlich carcinoma via triggering apoptosis and inhibiting proliferation/angiogenesis. Toxicol Appl Pharmacol. 2021;432:115767. doi: 10.1016/j.taap.2021.115767. PMID 34699866.
 - Zbidah M, Lupescu A, Shaik N, Lang F. Gossypol-induced suicidal erythrocyte death. Toxicology. 2012;302(2-3):101-5. doi: 10.1016/j.tox.2012.09.010, PMID 23041711.

9. Gao Y, Tai W, Wang X, Jiang S, Debnath AK, Du L. A gossypol derivative effectively protects against Zika and dengue virus infection without toxicity. *BMC Biol.* 2022;20(1):143. doi: 10.1186/s12915-022-01344-w, PMID 35706035.
10. Keshmiri Neghab H, Goliaei B. Therapeutic potential of gossypol: an overview. *Pharm Biol.* 2014;52(1):124-8. doi: 10.3109/13880209.2013.832776, PMID 24073600.
11. Rao MV, Narechania MB. The genotoxic effects of anti-cancer drug gossypol on human lymphocytes and its mitigation by melatonin. *Drug Chem Toxicol.* 2016;39(4):357-61. doi: 10.3109/01480545.2015.1039646, PMID 27071859.
12. Conceicao AA, Soares Neto CB, Ribeiro JAA, Siqueira FG, Miller RNG, Mendonca S. Development of an RP-UHPLC-PDA method for quantification of free gossypol in cottonseed cake and fungal-treated cottonseed cake. *PLOS ONE.* 2018;13(5):e0196164. doi: 10.1371/journal.pone.0196164, PMID 29791447.
13. Malyuchenko NV, Kotova EY, Kirpichnikov MP, Studitsky VM, Feofanov AV. PARP1 binding to DNA breaks and hairpins alters nucleosome structure. *Moscow Univ Biol Sci Bull* 2019;74(3):158-62. doi: 10.3103/S0096392519030076.
14. Zhang YS, Yuan J, Fang ZZ, Tu YY, Hu CM, Li G. Gossypol exhibits a strong influence towards UDP-glucuronosyltransferase (UGT) 1A1, 1A9 and 2B7-mediated metabolism of xenobiotics and endogenous substances. *Molecules.* 2012;17(5):4896-903. doi: 10.3390/molecules17054896, PMID 22543504.
15. Balaban AT. Topological indices are based on topological distances in molecular graphs. *Pure Appl Chem.* 1983;55(2):199-206. doi: 10.1351/pac198855020199.
16. Popov VI. ChemicPen. Certificate of official registration of software No. 2005612073. Rospatent. 2005.
17. Popov VI. ChemicDescript. Certificate of official registration of software No. 2003612305. Rospatent. 2003.
18. ChemicPen CCPC. Available from: <https://cetramax-chemicpen>. [Last accessed on 01 Jul 2022]
19. Borodina YV, Filimonov DA, Poroikov VV. Computer-aided prediction of prodrug activity using the PASS system. *Pharm Chem J.* 1996;30(12):760-3. doi: 10.1007/BF02218831.
20. Koldina AM, Uspenskaya EV, Borodin AA, Pleteneva TV, Syroeshkin AV. Light scattering in research and quality control of deuterium-depleted water for pharmaceutical application. *Int J App Pharm.* 2019;11(2):271-8. doi: 10.22159/ijap.2019v11i5.34672.
21. Uspenskaya EV, Pleteneva TV, Syroeshkin AV, Kazimova IV, Elizarova TE, Odnovorov AI. Role of stable hydrogen isotope variations in water for drug dissolution managing. *Curr Issues Pharm Med Sci.* 2020;33(2):94-101. doi: 10.2478/cipms-2020-0017.
22. Syroeshkin AV, Uspenskaya EV, Pleteneva TV, Morozova MA, Maksimova TV, Koldina AM. Mechanochemical activation of pharmaceutical substances as a factor for modification of their physical, chemical and biological properties. *Int J App Pharm.* 2019;11(4):118-23. doi: 10.22159/ijap.2019v11i3.32413.
23. Michel D. Simply conceiving the arrhenius law and absolute kinetic constants using the geometric distribution. *Phys. A Stat Mech Appl.* 2013;329(5):4258-64.
24. Peleg M, Normand MD, Corradini MG. The Arrhenius equation revisited. *Crit Rev Food Sci Nutr.* 2012;52(9):830-51. doi: 10.1080/10408398.2012.667460, PMID 22698273.
25. Wang X, Howell C, Chen F. Gossypol-a polyphenolic compound from cotton plant. *Adv Food Nutr Res.* 2009;58(5):215-63.
26. Shaik B, Agrawal VK, Manikpuri AD, Khadikar PV. Prediction of ¹³C NMR chemical shift sum using topological indices: role of recently introduced Balaban F and G Indices. *Interdiscip Sci.* 2015;7(3):83-92.
27. Zeng Y, Ma J, Xu L, Wu D. Natural product gossypol and its derivatives in precision cancer medicine. *Curr Med Chem.* 2019;26(10):1849-73. doi: 10.2174/0929867324666170523123655, PMID 28545375.
28. Verma S, Kumar D, Kumar G, Singh AP. Impending contraceptives that might be a positive methodology towards the male contraception. *Int J App Pharm.* 2022;14(4):23-34. doi: 10.22159/ijap.2022v14i2.43941.
29. Borovskaya TG. Safety of the Russian antiviral drug Kagocel. *Ter Arkh.* 2017;89(11):93-9. doi: 10.17116/terarkh2017891193-99, PMID 29260752.
30. Odnovorov AI, Grebennikova TV, Pleteneva TV, Garaev TM, Uspenskaya EV, Khodorovich NA. Physicochemical properties and biological activity of the new antiviral substance. *Int J App Pharm.* 2020;12(1):237-42. doi: 10.22159/ijap.2020v12i4.38136.
31. Abdelrahman SA, Yassin AA, Mirghani MES, Bashir NH. Determination of gossypol in Hamid and bt (seeni 1) cottonseed oil using fourier transform infrared spectroscopy. *Borneo J Pharm.* 2020;3(4):227-34. doi: 10.33084/bjop.v3i4.1592.
32. Uspenskaya EU, Anfimova EV, Pleteneva TV. Kinetics of active pharmaceutical ingredient solubility in water with different hydrogen isotopic content. *Pharmaceutical Sciences* 2018;80(2):318-24. doi: 10.4172/pharmaceutical-sciences.1000360.
33. Uspenskaya EV, Pleteneva TV, Hanh PM, Kazimova IV. Assessment of biology activity of the peeling substances by the physicochemical approaches on the spirostomum ambiguum cell model. *Int J Pharm Pharm Sci.* 2021;13(1):82-6.